

COMPARATIVE INVESTIGATIONS OF THE ABSORPTION AND FLUORESCENCE SPECTRA OF TETRAPYRIDYLPORPHYRINE AND Zn(II) TETRAPYRIDYLPORPHYRINE

Eugenia Fagadar-Cosma^{a*}, Corina Enache^a, Ileana Armeanu^a, Gheorghe Fagadar-Cosma^b

^a Institute of Chemistry –Timisoara of Romanian Academy, M. Viteazul Ave, No. 24,
300223-Timisoara, Romania

^b"Politehnica" University, T. Lalescu Street, No. 2, 300223-Timisoara, Romania

5,10,15,20-Tetrakis(4-pyridyl)-21H,23H-porphine (TPyP) molecules easily self-assemble into large highly ordered domains. Their photophysical properties could be strongly affected by changes in their aggregation state. The present study is concerned about the synthesis and UV-vis, FT-IR, ¹H-NMR and solid-state ¹³C-NMR spectroscopic characterization of TPyP. Among the investigations, one focus is about the comparative study of the absorption and fluorescence spectra of meso-tetrapyrrolic porphyrine and its Zn complex in diverse solvents, various concentrations and different pH conditions.

(Received March 15, 2007; accepted March 22, 2007)

Keywords: Porphyrin, Zn-porphyrin, UV-vis, Fluorescence spectra, ¹H-NMR, Solid-state ¹³C-NMR

1. Introduction

Because they strongly absorb light, porphyrins, have been gained the interest of scientists in physics, chemistry and medicine in the last two decades. It has been known that many porphyrins are being used as photosensitizers in photodynamic therapy [1], for the treatment of tumors and malignant tissues [2] in combination with electromagnetic radiation or radioactive emissions.

Their high optical absorption in visible region of the solar spectrum also determined a great deal of interest in the photovoltaic properties of phthalocyanines and porphyrins, as inexpensive materials for solar cells.

New types of three-layered organic photovoltaic cells suggest an improvement over two-layered cells, because the codeposited interlayer [3], has been found to act as an efficient carrier photogeneration layer. A large number of fullerene-porphyrin dyads in a variety of arrangements have been synthesized in order to gain control over the electronic coupling in the photophysical processes between the donor, usually a Zn-metalloporphyrin [4] and acceptor. A system, made of four perylene diimides connected to central zinc 5,10,15,20-tetraphenylporphyrin [5], as electron donor, self-assembles into ordered nanoparticles, both in solution and in the solid state and exhibit photoinduced charge separation and charge transport, which demonstrates the feasibility of the supramolecular approach.

The photophysical properties of the tetrapyrrolic sensitizers could be highly affected by changes in their aggregation state. Formation of aggregates brings changes in the absorption spectra of porphyrins [6]. It is known from the experimental investigations that medium in cancerous tissues is often more acidic than in normal tissues [7]. A hydrophilic molecule accumulates in cells mainly in lysosomes [8], where medium is acidic. Dicationic species of TPyP are formed at the values of pH, characteristic for acidic medium. Aggregated species can facilitate important processes such as light harvesting antenna and the primary charge-separation steps in photosynthesis.

TPyP molecules easily self-assemble into large highly ordered domains. Lateral intermolecular interactions control the packing of the layer, while its orientation is induced by the

* Corresponding author: efagadar@yahoo.com

link with the substrate. In order to improve the producing of functional nanoscale molecular devices based on functional supramolecular structures, building of self organized systems are one of the main purposes of nanotechnology research.

The molecular self-assemblies of zinc meso-tetra(4-pyridyl)porphyrin (ZnTPyP) with the assistance of a surfactant were reported to give hexagonal nanoprism. Furthermore, the one-dimensional (1D) assembly can self-organize into a three-dimensional (3D) superstructure through the simple evaporation of the solvent.

In this model, the zinc atom at the center of ZnTPyP is six-coordinated to four pyrrole nitrogens of porphyrin core and to two pyridyl N-atoms of other porphyrins approaching from both side of the molecular framework. Each porphyrin monomer is thus strongly linked to four neighboring porphyrin units. The structure can be also described as one consisting of a circular hexameric cage crosslinked by axial coordination of pyridyl ligands, which propagates in three different directions of the trigonal lattice. A notable feature of such a structure is that the center of the hexameric cage has a large cavity of about 19 Å with a functional pyridine window where water molecules may be ligated through hydrogen bondings. The adjacent circular hexameric cage arrays interpenetrate each other in the crystal structure and are “glued” by noncovalent π - π interactions between porphyrin molecules, which may be further stabilized by hydrogen bridges [9].

The present study is concerned about the synthesis and UV-vis, FT-IR, $^1\text{H-NMR}$ and solid-state $^{13}\text{C-NMR}$ spectroscopic characterization of TPyP. Among the investigations, one focus is the comparative study of the absorption and fluorescence spectra of tetrapyridylporphyrine and Zn-tetrapyridylporphyrine in diverse conditions.

2. Experimental

Reagents: Spectral grade solvents were used for all measurements, which were carried out at room temperature. Stock solutions of sensitizer (10^{-3} M) were prepared by dissolving crude TPyP in chloroform. Further dilution was carried out directly before the measurements.

Apparatus: FT-IR (JASCO 430 FT-IR, KBr pellets) spectra were carried out, in the 4000-400 cm^{-1} range. UV-visible spectra were recorded on a UV/VIS PERKIN ELMER, LAMBDA 12 spectrometer. Fluorescence spectra were recorded in THF and in aqueous solution on a PERKIN ELMER apparatus in a 1 cm cuvette. The following excitation wavelengths were chosen: $\lambda_{\text{ex}} = 395$; 410; 417; 435 nm. Excitation spectra were collected at the wavelengths: $\lambda_{\text{em}} = 603$ and 656 nm. $^1\text{H-NMR}$ spectrum was registered on a 400 MHz Bruker spectrometer in CDCl_3 and chemical shifts are reported relative to internal TMS (0.0 ppm). The HPLC analysis were performed on a JASCO apparatus equipped with NUCLEOSIL C18 nonpolar column, and on KROMASIL SI 100 5 μm polar column, 240x4 mm with MD 1510 detector, at ambient temperature.

Preparation of TPyP, was done according to literature data [10]: A mixture of 9.41 ml (100 mmol) of 4-pyridinecarboxaldehyde and 13 ml (100 mmol) propionic anhydride was dissolved in 300 ml propionic acid and 6.93 ml (100 mmol) pyrrole dissolved in 100 ml of propionic acid, was added dropwise to the mixture heated to reflux, for 1/2 h. The whole reaction mixture was refluxed for over 2h. After cooling to room temperature, the solvent was evaporated to dryness, and the oily residue was repeatedly washed with hot water, neutralized by aqueous ammonia (25%), and washed again with hot water. The purple solids obtained by this procedure were filtered and dried. The dry solid material was treated with three portions of 80 ml of dichloromethane, each followed by filtration. To the combined organic phases, 15 g of basic alumina (Brockman activity grade II) were added, and the solvent was evaporated to dryness. Separation of 5,10,15,20-tetra(4-pyridyl)porphyrin was achieved by column chromatography, using as eluent a mixture of chloroform, dichloromethane and ethanol.

Preparation of ZnTPyP, was done according to literature data [11] by using 0.108 g (0.175 mmol) TPyP and 0.173 g (0.87 mmol) Zn acetate, heated to reflux for 2 hours in a mixture of 20 ml glacial acetic acid and 20 ml DMF. After cooling, the crystals are washed with water to remove the excess of Zn acetate and after drying it could be purified by column chromatography using as stationary phase Al_2O_3 and as eluent a mixture consisting of 95% CHCl_3 and 5% methanol.

3. Results and discussion

The main spectrometric characteristics of free base porphyrin are given below: **5,10,15,20-tetrakis(4-pyridyl)-21H,23H-porphine (TPyP)** violet crystals, $\eta = 11\%$, FT-IR(KBr), cm^{-1} : 3306.36; 3098.87; 3024.8; 1589.06; 1546.63; 1404.89; 1349.93; 1068.37; 975.80; 884.20; 798.38; 724.13; 656.64; 528.4. $^1\text{H-NMR}$ (CDCl_3 , 400 MHz), δ , ppm: -2.916 (s, 2H, NH), 8.155-8.169 (dd, 8H, 3,5 H- Ph (*meso*)), 8.873 (s, 8H, 2,6 H- Ph (*ortho*)), 9.062-9.076 (d, 8H, β -H). UV-Vis (MeOH) – λ_{max} (log ϵ): 411.96 (5.61); 509.00 (4.84); 537.99 (4.77); 584.11 (4.77); 642.00 (4.77). UV-Vis (THF) - λ_{max} (log ϵ): 415.04 (5.66); 511.03 (4.43); 543.34 (3.95); 587.95 (3.95); 642.95 (3.95).

The FT-IR spectrum of TPyP is in complete agreement with the structure. The absorptions at 3306 and 975 cm^{-1} are attributed to stretching and bending vibrations of N-H and C-N, respectively, which are the characteristic absorptions of porphyrin free base. The bands in the range 1500 - 1600 cm^{-1} are due to stretching vibration of C = C in the pyridyl aromatic ring. The intense absorption band at 798 cm^{-1} is attributed to the vibration of C-H bond from pyrrole.

The $^1\text{H-NMR}$ spectrum of TPyP presents all the expected signals from a symmetrical *meso*-substituted compound in which a significant diminution of the current of cycle causes the shielding of β pyrrolic protons and the unshielding of internal NH protons. So the signal corresponding to NH pyrrolic protons appears as broad singlet at -2.916 ppm and the signal for β pyrrolic protons is located at 9.062-9.076 ppm. The signals for phenyl protons are to be seen as two doublets at 8.155-8.169 ppm for the eight 3,5 H-Ph (*meso*) protons, and in the range of 8.873 ppm for the eight 2,6 H-Ph (*ortho*) protons.

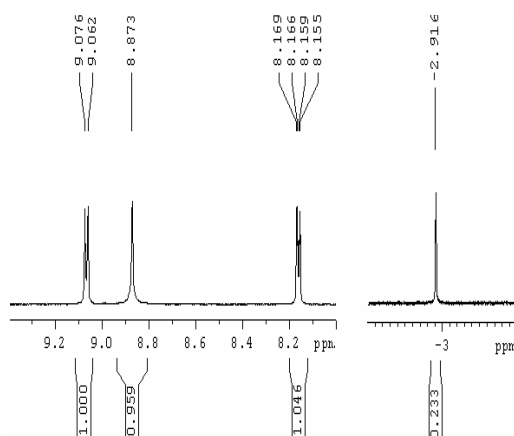


Fig. 1. $^1\text{H-NMR}$ Spectrum of TPyP in CDCl_3 .

The signals in $^{13}\text{C-NMR}$ of TPyP are large (about 300 Hz), five-eight times larger than in usual organic compounds (Fig. 2). This feature may be caused by the ring-currents and π - π interactions, which are supposed to be very strong. The signals in $^{13}\text{C-NMR}$ of TPyP are divided in some major regions. The α -pyrrolic carbons, very sensitive to electronic effects, gave the signal around 145 ppm. The β -pyrrolic carbons are resonating around 130 ppm and the *meso*-carbons between 95 ppm and 120 ppm. In case of solid state NMR symmetry duplication multiplies signal height, and gave the same line. In general, the solid-state $^{13}\text{C-NMR}$ spectra may differ from those obtained in solution both in the number of observed resonances as well as in their chemical shifts. When using the $^{13}\text{C-NMR}$ technique, a factor of importance is the intrinsically lower resolution of solid-state experiment, as compared with solution NMR [12]. Other factors are related to the structure of the molecule under observation in the solid phase. For example, nuclei that are chemically equivalent in solution may become nonequivalent in the solid due to crystal packing effect. An additional complication appears when some of the carbons being observed are attached to a ^{14}N , since the dipolar coupling $^{13}\text{C-}^{14}\text{N}$ cannot be completely removed and the ^{13}C resonances may appear broadened or split into an asymmetric doublet.

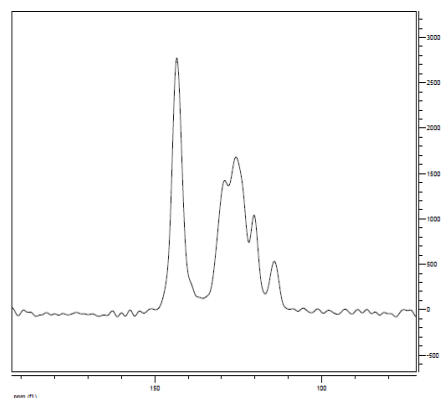


Fig. 2. Solid state ^{13}C -NMR Spectrum of TPyP in CDCl_3 .

As can be seen in Figs. 3 and 4, the absorption spectrum of TPyP comprises the π - π^* absorption bands characteristic of free-base etio type porphyrin. An intense near-UV Soret band with a peak around 412 nm in methanol, at 415 nm in THF and also with a slight shoulder at higher energy 381.5 nm, due to B(0,0) and B(0,1) electronic transitions, respectively, are to be seen. The Q bands are located in the visible spectral region around 510, 540, 585 and 642 nm.

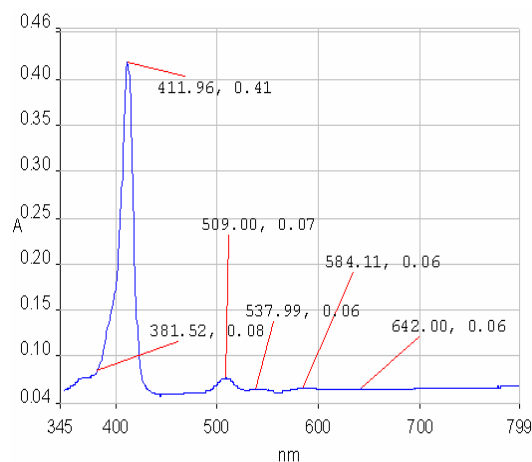


Fig. 3. UV-vis Spectrum of TPyP in methanol ($c=1 \times 10^{-6}\text{M}$).

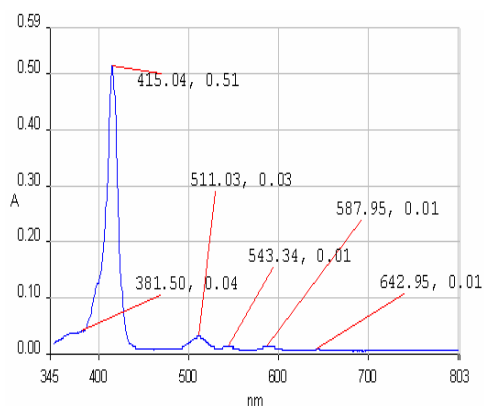


Fig. 4. UV-vis Spectrum of TPyP in THF ($1.1 \times 10^{-6}\text{M}$).

Mesotetrapyrridylporphyrin (TPyP) and its complexes are usually more stable to pH changes than the corresponding TPP analogues because the pyridyl substituents act as a sponge for surface protons. The equilibria involved in these processes are complex because of the relatively high pK of

the pyridyl substituents, and two different steps are involved in this case, the exterior protons are those attached to the pyridyl nitrogens while the interior ones are bonded to the pyrrole nitrogens.

At pH values below 3.5 the absorption spectrum of TPyP in the visible spectral region transforms into a two Q-band spectrum, composed of an intense absorption band over 650 nm, and a band around 602 nm of weaker intensity. From Fig. 5 it can be seen that the Soret band is red-shifted with more than 40 nm, with respect to that of spectrum in organic solvents, being situated to 456 nm.

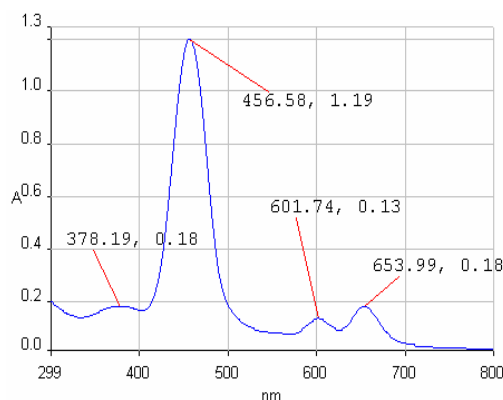


Fig. 5. The allure of the absorption spectra of TPyP in aqueous solution pH=3.5.

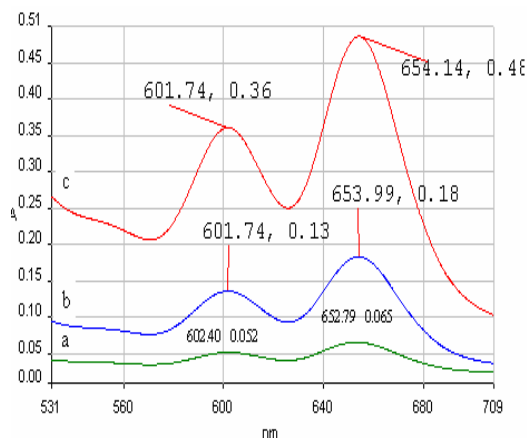


Fig. 6. The allure of the Q bands of TPyP in aqueous solution at different pH-values: 4 (a); 3.5 (b); 2 (c).

With increasing acidity to pH 2 and lower, two additional protons bond to the nitrogen atoms in the center of porphyrin ring, so that the partial positive charge is induced in the central part of the molecule. These changes in spectral allure might be attributed to the dication (H_2^+TPyP) generations, and are associated with an increase of the intensity of the last Q band (Figure 6). Literature data offers information about similar changes in absorption spectra which can be induced by varying the ionic strength of acidic solution of porphyrins and have been assigned to the formation of aggregates [13, 14].

The fluorescence excitation spectra are presented at different concentrations (Fig. 7) and were registered at the maximum value of λ emission = 656 nm. According to the decrease of concentration it can be seen that the lower energy Soret band at 440 nm, associated with J type aggregate mode, decreases gradually while the high-energy Soret band around 420 nm, associated with monomer, appears in very diluted systems [9]. The formation of the two paired porphyrin - electrons in the aggregates, is concordant with the observed band-shift and broadening in the UV-visible absorption spectrum of the aggregate [15].

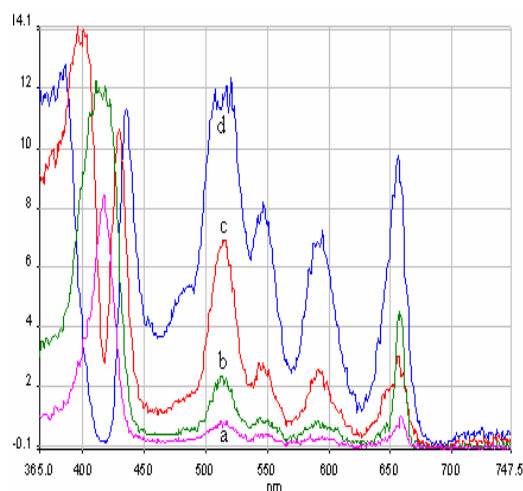


Fig. 7. Fluorescence spectra of TPyP in THF at different concentrations: $1.11 \cdot 10^{-6}$ M (a); $5.56 \cdot 10^{-6}$ M (b); $2.78 \cdot 10^{-5}$ M (c); $1.39 \cdot 10^{-4}$ M (d), $\lambda_{em}=656$ nm.

The fluorescence emission spectra recorded for TPyP samples of various concentrations in THF, and excited at the excitation wavelength of 420 nm are shown in Figure 8 (curve A). The spectrum of the dication, at pH=2, when excited at its Soret-band maximum, exhibited a broad band whose maximum is around 660 nm (curve B).

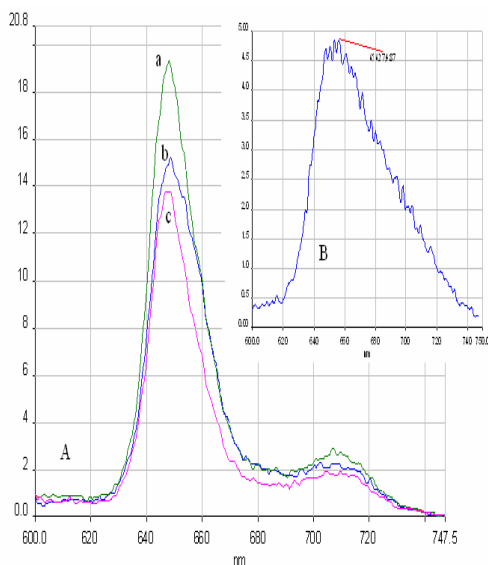


Fig. 8. Emission spectra of TPyP in THF of various concentrations: $1.39 \cdot 10^{-4}$ M (a); $2.78 \cdot 10^{-5}$ M (b); $5.56 \cdot 10^{-6}$ M (c); $\lambda_{ex}=420$ nm (curve A). The spectrum of the dication, in aqueous solution at pH=1.5 (curve B).

When the emission spectra were excited at different excitation wavelengths, it was put into evidence that the intensity of the emission spectra is in accordance with the magnitude of energy of the excitation (Fig. 9).

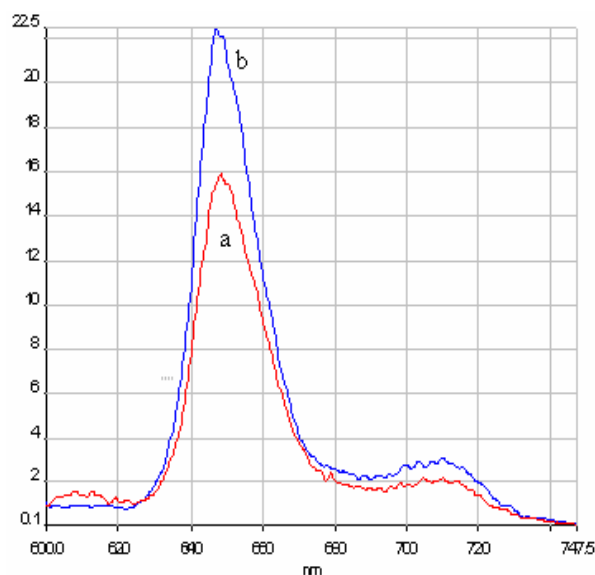


Fig. 9. Emission spectra of TPyP in THF at different excitation wavelengths: 395nm (b) and 431nm (a).

In comparison with TPyP, the Zn-metallated complex exhibits emission bands around 600 and 660 nm upon excitation at 395 nm, whereas the free base TPyP exhibits bands at 650 and 710 nm upon excitation at the same wavelength.

It seems clear that the 600 nm band is characteristic of the metallated complex (Figure 10).

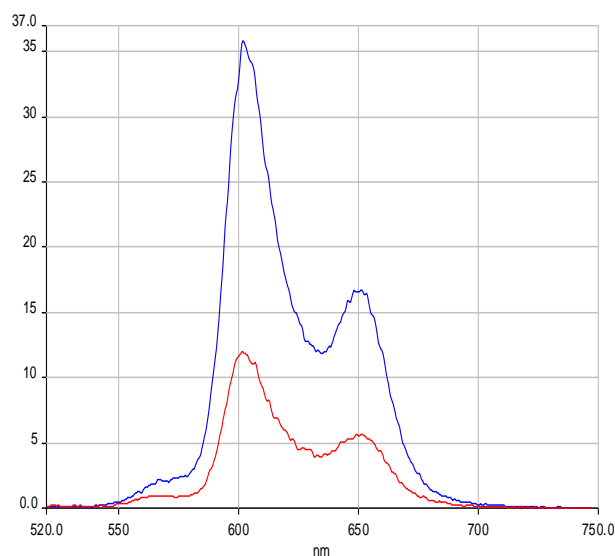


Fig. 10. Emission spectra of Zn-TPyP in THF at $\lambda_{ex}=395$ nm, at different concentrations: $1 \cdot 10^{-5}$ M (higher intensity); $1 \cdot 10^{-6}$ M (lower intensity).

The excitation spectra of Zn-TPyP in THF at the at emission wavelength of 603 nm presents the same significant differences from the porphyrin base as the differences registered in the UV-vis spectra (Figure 11). Instead of four Q bands in the TPyP excitation spectrum there are only two bands in the spectrum of ZnTPyP, but at the same concentration, their intensity is highly increased.

The same association process of the molecules is to be underlined if the concentration is equal or higher with $1 \cdot 10^{-5}$ M, producing the splitting of Soret band into two Lorentzian bands.

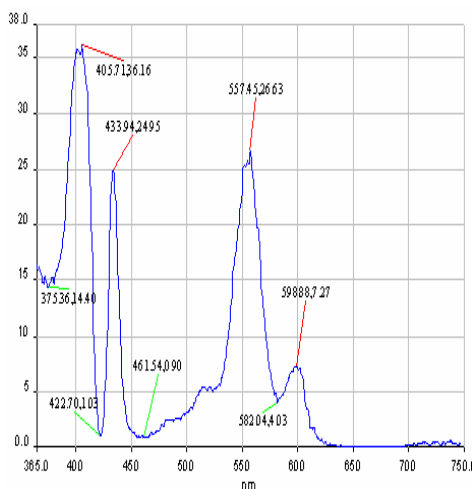


Fig. 11. The excitation spectra of Zn-TPyP in THF ($c=1 \times 10^{-5} \text{M}$) $\lambda_{em}=603 \text{ nm}$.

4. Conclusions

The present study was concerned about the synthesis and UV-vis, fluorescence, FT-IR, ^1H -NMR and solid-state ^{13}C -NMR spectroscopic characterization of TPyP. Among the investigations, one focus is the comparative investigations of the absorption and fluorescence spectra of meso-tetrapyrroldiporphyrine and its Zn complex in diverse conditions.

At pH values below 3.5 the absorption spectrum of TPyP in the visible spectral region transforms into a two Q-band spectrum, composed of an intense absorption band over 650 nm, and a band around 602 nm of weaker intensity, and the Soret band is significantly red-shifted.

These changes in spectral allure might be attributed to the dication (H_2^+TPYP) generations, and are associated with an increase of the intensity of the last Q band.

In the fluorescence excitation spectra in accordance with the decrease of concentration it can be seen that the lower energy Soret band at 440 nm, associated with J type aggregate mode, decreases gradually while the high-energy Soret band around 420 nm, associated with monomer, reappears in much diluted systems.

In comparison with TPyP the Zn-metallated complex exhibits emission bands around 600 and 660 nm upon excitation at 395 nm, whereas the free base TPyP exhibits bands at 650 and 710 nm upon excitation at the same wavelength.

Instead of four Q bands in the TPyP excitation spectrum there are only two bands in the spectrum of ZnTPyP, but at the same concentration, their intensity is highly increased.

Acknowledgement

Authors are grateful to MATNANTECH-Programme because this work has been partially supported by CEE X Projects No. 38/2005 and 48/2006.

References

- [1] T. J. Dougherty, C. J. Gomer, B. W. Henderson, G. Jori, D. Kessel, M. Korblik, J. Moan, Q. Peng, Photodynamic Therapy. *J. Natl. Cancer Inst.* **90**, 889 (1998).
- [2] D. Aviezer, S. Cotton, M. David, A. Segev, N. Khaselev, N. Galili, Z. Gross, A. Yaron, *Cancer Research* **60**, 2973 (2000).
- [3] S. Antoine, V. Ruxandra, L. Tugulea, V. Gheorghe, D. Ionascu, *J. Phys. III France* **6**, 1133 (1996).
- [4] D. M. Guldi, *Pure Appl. Chem.* **75**, 1069 (2003).
- [5] T. Van der Boom, R. T. Hayes, Y. Zhao, P. J. Bushard, E. A. Weiss, M. R. Wasielewski, *J. Am. Chem. Soc.* **124**, 9582 (2002).

- [6] T. K. Chandrashekar, H. van Willigen, M. H. Ebersole, *J. Phys. Chem.* **88**, 4326 (1984).
- [7] J. P. Keene, D. Kessel, E. J. Land, R. W. Redmod, T. G. Truscott, *Photochem. Photobiol.* **43**, 117, 1986).
- [8] J. M. Wessels, W. Strauss, H. K. Seidlitz, A. Rück, H. Schneckenburger, *J. Photochem. Photobiol. B. Biol.* **12**, 275 (1992).
- [9] J. S. Hu, Y. G. Guo, H. P. Liang, L. J. Wan, L. Jiang, *J. Am. Chem. Soc.* **127**, 17090 (2005).
- [10] D. Aviezer, S. Cotton, M. David, A. Segev, N. Khaselev, N. Galili, Z. Gross, A. Yayon, *Cancer Research* **60**, 2973 (2000).
- [11] E. B. Fleischer, *Inorg. Chem.* **3**, 493 (1962).
- [12] L. Frydman, A. C. Olivieri, L. E. Diaz, A. Valasinas, B. Frydman, *J. Am. Chem. Soc.* **110**, 5651 (1988).
- [13] D. L. Akins, S. Özelik, H. R. Zhu, C. Guo, *J. Phys. Chem.* **100**, 14390 (1996).
- [14] R. Augulis, V. Snitka, R. Rotomkis, *Solid State Phenomena* **97-98**, 191 (2004).
- [15] D. M. Chen, Y. H. Zhang, T. J. He, F. C. Liu, *Spectrochimica Acta Part A* **58**, 2291 (2002).